Non-Arrhenius behavior: Influence of the crystallinity on lifetime predictions of polymer materials used in the cable and wire industries

Camille Blivet, Jean-François Larché, Yaël Israëli, Pierre-Olivier Bussière

Version of Record: https://www.sciencedirect.com/science/article/pii/S0141391022000763
Manuscript_767ffbcb4e0bf6eb0f5c489084e6a3f8

Non-Arrhenius behavior: influence of the crystallinity on lifetime predictions of polymer materials used in the cable and wire industries

Camille Blivet[1], Jean-François Larché[2], Yaël Israëli[1], Pierre-Olivier Bussière[1]

[1)] Université Clermont Auvergne, CNRS, Clermont Auvergne INP, ICCF, F-63000 Clermont-Ferrand, France

[2)] Nexans Research Center (NRC), 53 rue Saint-Jean-De-Dieu, 69007 Lyon, France

*Corresponding authors:

I.C.C.F, UMR 6296 - Institut de Chimie de Clermont-Ferrand, Université Clermont Auvergne - CNRS - SIGMA Clermont Campus des Cézeaux - 24, avenue Blaise Pascal - TSA 60026 - CS 60026 63178 Aubière Cedex, France. E-mail address: pierre-olivier.bussiere@sigma-clermont.fr (P.-O. Bussière).

Nexans Research Center (NRC) – 53 rue Saint-Jean-De-Dieu, 69007 Lyon, France – Email address: jean_francois.larche@nexans.com (J.-F. Larché).

Abstract

Thermo-oxidation (50 – 160 °C) of two polymer materials widely used as electrical insulators in cable systems was studied: a peroxide cross-linked polyethylene (XLPE) and a peroxide cross-linked ethylene propylene diene monomer (XLEPR). The materials were characterised by infrared spectroscopy measurements and tensile testing. Arrhenius treatment was applied to the data, using the relative conversion rate methodology and the shift factor methodology over the entire temperature range. The physical state of the material (semi-crystalline or amorphous) was shown to have no influence on the Arrhenius behaviour for two reasons: (a) no Arrhenius deviation was observed at the melting temperature of the polyethylene matrix (117 °C) and (b) an Arrhenius deviation was observed at the same temperature (50 °C) for the two polymers, despite their difference in terms of crystallinity and physical state at the ageing temperatures studied. This deviation at low temperature led to large overestimations of lifetime predictions for both materials (28 % for XLPE and 78 % for XLEPR).

Keywords: Cross-linked polyolefins, thermo-oxidation, crystallinity, Arrhenius law, non-linearity, lifetime prediction.

1. Introduction

For many years, ensuring the durability of materials has been a major concern in various fields, such as the structures and buildings, automotive and aeronautics, and packaging industries, Materials are submitted to different environmental conditions and substances during their use, such as oxygen, light, heat, radiation or humidity. This induces degradation of the material, which then fails to satisfy the requirements for its application. The cable industry is particularly interested in assessing the durability of materials used in nuclear power plants, rolling stock or photovoltaic applications. Polymers such as cross-linked polyethylene (PE) and cross-linked ethylene propylene diene monomer (EPR) are widely used as insulating materials. In such applications, temperature elevation is generally the main stress to which the polymers are subjected during their operation, and it leads to thermo-oxidation. The consequences of thermo-oxidation for PE and EPR were reported in the literature: they include modification of the chemical structure [1–6], changes in the macromolecular architecture and the cross-linked network [7–12], and modification of mechanical properties. Recently, the present authors have used a multi-scale analysis to study the structure-properties relationships capable of correlating chemical and mechanical results [13].

When durability problematics are discussed, the main challenge for industry is the determination of lifetimes for the materials used. There are economic and regulatory issues linked to equipment maintenance as well as strategic issues behind this challenge. In polymer ageing, the prediction of lifetime has been based for many years on the Arrhenius law, which results in a proportional relationship between rate constant of the thermo-oxidation k and the inverse of the absolute temperature $\frac{1}{T}$, such as:

$$\mathrm{k} = \mathrm{A} \times \exp\left(\frac{-Ea}{RT}\right) \qquad \textit{(Eq. 1)}$$

where A is a pre-exponential factor, E_a is the activation energy and R is the gas constant. Accelerated thermal ageing at temperatures above the operating temperature of the material is

used to accelerate the physicochemical phenomena. The results are then extrapolated to the working temperature of the materials. Generally, a specific property of the material is monitored to account for the degradation. Thus, it is possible to predict the behaviour of the material at the temperature of interest.

The Arrhenius methodology for lifetime prediction involves the following hypotheses:

- From a kinetic point of view, the thermo-oxidation phenomenon is assimilated as an elementary process, which has a single Arrhenius temperature dependence [14,15]. As has been known for a long time, thermo-oxidation is composed of several reaction steps. Experts on the ageing of materials have assumed that the overall thermo-oxidation mechanism, despite its complexity, should obey the Arrhenius law with one "global" or "apparent" activation energy;
- It is assumed that the activation energy is constant over the temperature range. This means that there is no change in the reaction mechanism between the studied accelerated temperature range and the temperature of interest for which a prediction is needed.

The Arrhenius methodology has, for years, led to many controversies. Numerous examples of the nonlinearity of the law over the studied temperature range have already been reported in the literature. In a work of 2005, Celina *et al.* [16] did an extensive review of the literature of previous evidence of non-Arrhenius behaviours. Cases of non-linearities have often been reported for polyethylene and polypropylene. For polypropylene, Tamblyn and Newland [17] were among the first to report an Arrhenius deviation for the material thermally aged between 70 °C and 160 °C, leading to an overestimation of the lifetime (one week from the experiment versus five years from the extrapolation). In 1981, Billingham *et al.* [18] reported an Arrhenius deviation for an isotactic polypropylene occurring in the polymer melting region. They reported induction periods much longer than predicted from the melt state region data, which they attributed to the restriction of the mobility of the polymeric radicals imposed by the crystallisation process.

For polyethylene, in 1986, Kramer *et al.* [19] reported an Arrhenius discontinuity near 150 °C in the case of the thermo-oxidation of two differently stabilised cross-linked polyethylenes. The authors attributed the deviation to an unspecified mechanistic change (for the highly effective antioxidant system) and to the melting temperature of the polyethylene matrix (for the less effective antioxidant system). In other works, Howard *et al.* [20,21] reported an

overestimation of the lifetime for a low-density polyethylene when extrapolating high-temperature of differential thermal analysis (DTA) data (140 – 220 °C) below 80 °C. The authors attributed this deviation to lower solubility of stabilisers in polyethylene below this critical temperature, inducing the diffusion and loss of the stabiliser in the atmosphere. The same conclusion has been reported by Langlois *et al.* [22] for a cross-linked polyethylene for which a deviation has been observed near the melting point of the polyethylene. The authors assigned this deviation to changes in antioxidant solubility when crossing this transition temperature. Furthermore, many studies were interested in assessing the diffusion and solubility behaviour of antioxidants in polyolefins [23–29]. In these studies, diffusion and solubility coefficients were shown to be smaller at lower temperatures, and, more interestingly, that these coefficients did not obey the Arrhenius law. From a compilation of literature data and their own work, Khelidj *et al.* [30] reported an Arrhenius deviation for polyethylene occurring at 80 °C. They proposed a kinetic model able to explain this deviation based on peroxy radical diffusion, which would be higher above this temperature, thus restraining the termination step of the thermo-oxidation chain reaction.

Diffusion-limited oxidation problematics were also proposed as an explanation for Arrhenius deviations [31–35]. It is therefore noticed that many justifications have been provided by the ageing community to tentatively explain the observed Arrhenius deviations, leading to some controversies. These observed deviations shown at certain temperatures are generally explained by a difference in the chemical mechanism, by a diffusion-limited oxidation process, by polymer physical changes (crystallinity), or by the presence of stabilisers (and their diffusion or solubility), leading to erroneous lifetime predictions.

In this work, in order to investigate the influence of crystallinity on lifetime prediction using the Arrhenius law, thermo-oxidation of cross-linked PE and EPR, with different morphological state (crystallinity), was carried out at six ageing temperatures ranging from 50 to 160 °C. Ageing characterisation was carried out using infrared spectroscopy measurements and tensile tests. The Arrhenius law was used to determine the activation energies of thermo-oxidation. One of the particularities of this paper is the use and critical comparison of two approaches. The first is the “relative conversion rate approach”, which allows us to determine the evolution of activation energies during the progress of thermo-oxidation, as monitored by infrared spectroscopy and tensile tests. The second is the “shift factor approach”, which is based on the time-temperature principle and was proposed initially by Gillen and co-workers [31,33,34,36,37]. The novelty of this work is the achievement of thermal ageing at a low

temperature (50 °C), in order to compare the results obtained from the experience with the results obtained from Arrhenius predictions using extrapolations from data at high temperatures. The temperature range studied is thus very large (50 – 160 °C). The study of low temperatures (50 – 70 °C) is of particular interest because they are close to those that the material will experience during natural ageing in normal use (in nuclear power plants, for example).

2. Experimental Section

2.1. Materials

Two materials were studied in this work. The first was a linear low-density polyethylene (LLDPE) produced by Ineos ($T_{melting}$ = 105 – 125 °C, density = 0.93 kg.m^{-3}, melt flow index MFI = 3.3 g/10 min). The second was an ethylene-propylene diene monomer copolymer (EPDM) produced by Exxon Mobil (density = 0.87, Mooney viscosity ML (1+4 at 125 °C) = 25). The ethylene content is 77.0 wt%, and the vinyl norbornene (VNB) content is 0.9 wt%. In the rest of the work, this material is referred to as EPR because of the very low content of diene. Both materials were cross-linked using 2 wt% dicumyl peroxide (DCP) from Arkema.

The two polymers were processed with the cross-linking agent for 7 min using an internal mixer with a volume of 300 cm^3 at temperatures of 125 °C for PE and 95 °C for EPR. The materials were then processed with an extruder. The samples were then compression-moulded at 180 °C for crosslinking under a pressure of 18 tons for 9.5 min for PE and 8.5 min for EPR. Sheets of 1.0 ± 0.1 mm and films of 200 ± 10 µm thickness were obtained with this protocol. Cross-linked PE and cross-linked EPR are referred to as XLPE and XLEPR, respectively, in this work.

2.2. Thermal ageing conditions

Thermal ageing was performed using natural convection ovens operating at 50 °C, 70 °C, 90 °C, 120 °C, 140 °C and 160 °C. The oven temperature was controlled before and during the tests, with a tolerance of ± 1 °C. According to the International Electrotechnical Commission (IEC) 60216-4-2 international standard [38], air renewal rates must be set between 5 and 20 per hour: in this work, the air renewal rate was set between 16 and 20.

2.3. Caracterisation techniques

2.3.1. Infrared spectroscopy

Infrared spectra were recorded in transmission mode on 200 µm thick films using a Thermo Scientific Nicolet 6700 spectrometer, with 32 scans and a 4 cm^{-1} resolution. The band at 2019 cm^{-1} associated with the twisting of CH_2 and which the intensity did not change with ageing, was used as a reference peak [39–42] and allowed for a thickness correction for the different tested films.

2.3.2. Tensile tests

Mechanical tensile testing was performed according to international standard IEC 60811-501 [43] at room temperature, using a Zwick Z010 machine with a 500 N load cell. The crosshead speed was 250 $mm.min^{-1}$ and the displacement was measured using a mechanical extensometer in the central part of the specimen. Five dumbbell-shaped test specimens of 1 mm thickness were tested for each ageing time.

2.4. Determination of a relative conversion rate α

To quantitatively characterise the progress of polymer degradation, the term α was defined as the relative conversion rate of the thermo-oxidation reaction, and it can vary from 0 to 1 or 0 % to 100 %, as in:

$$\alpha_s\ [\%] = \frac{P_t - P_0}{P_{max} - P_{t0}} \times 100 \qquad \textit{(Eq. 2)}$$

where P_t is the "quantity" or "property" of the material at time t, P_0 is the "quantity" or "property" at t=0, P_{max} is the chosen extremum property level, which can be assimilated to an "end-of-life" criterion (or to a maximum property level measured), and P_{t0} is the initial value of the property at t=0. This relative conversion rate can be determined from different characterisation techniques, such as those mentioned above. For example, α can be defined from infrared spectroscopy measurements, as in the work of Musto *et al.* [44]. In our case, a relative conversion rate denoted as α_s was linked to the formation of the main oxidation product, i.e., ketones for XLPE and carboxylic acids for XLEPR, and especially to the absorbance $\Delta A = A_t - A_0$ at 1720 cm^{-1}, as in:

$$\alpha_s\ [\%] = \frac{A_t - A_0}{\Delta A_{max} - \Delta A_{t0}} \times 100 \qquad \textit{(Eq. 3)}$$

where A_t is the absorbance at 1720 cm^{-1} at time t, A_0 is the absorbance at 1720 cm^{-1} at t=0, ΔA_{max} is the maximum level of absorbance chosen for data processing and ΔA_{t0} is the initial

absorbance at t=0, which is by definition equal to 0. ΔA_{max} was initially chosen at 2 so that α_s = 0 % would correspond to the end of the induction period, defined as the first measurable and significant increase in the absorbance, and α_s = 1 would correspond to the criterion ΔA = 2. Between ΔA = 0 and ΔA = 2, the absorbance scale was cut into 10 parts so that α_s = 10 % would correspond to ΔA = 0.2, α_s = 20 % to ΔA = 0.4, α_s = 30 % to ΔA = 0.6, etc.

We also defined a relative conversion rate denoted as α_m, which was linked to the loss of the mechanical properties, and especially to the elongation at break property (EAB), as in:

$$\alpha_m[\%] = \frac{EAB_t - EAB_0}{EAB_{max} - EAB_0} \times 100 \qquad \textit{(Eq. 4)}$$

where EAB_t is the elongation at break at time *t*, EAB_0 is the initial elongation at break at t=0 (490 % for XLPE), EAB_{max} is the maximum level of elongation at break chosen for data processing and EAB_0 is the initial elongation at break at t=0 (490 %). EAB_{max} was initially chosen at 50 %.

3. Results and Discussion

3.1. Determination of the activation energy in the temperature range 70 – 160 °C

3.1.1. Application of the relative conversion rate α methodology

3.1.1.1. Infrared spectroscopy measurements

The purpose of this part is to determine the activation energy of the thermo-oxidation reaction versus the "relative conversion rate" of the thermo-oxidation reaction, using spectroscopic measurements.

The formation of XLPE oxidation products during thermo-oxidation occurring between 70 °C and 160 °C was monitored by infrared spectroscopy. The spectra and results were reported in a previous paper [13]. The kinetics of the formation of the main oxidation products, i.e., ketones exhibiting a peak at 1720 cm^{-1}, were studied at the five studied temperatures and the data are displayed in Figure 1 (a).

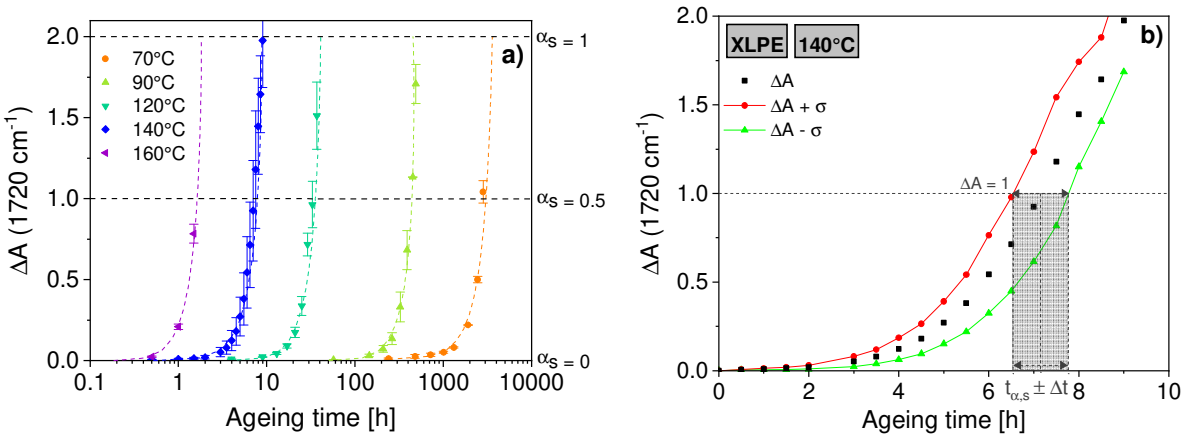

Figure 1: (a) Kinetic evolution of infrared absorbance $\Delta A = A_t - A_{t=0}$ at 1720 cm^{-1} for thermo-oxidation of XLPE at five temperatures (70 – 160 °C); (b) Example of the determination of the time $t_{\alpha,s} \pm \Delta t$ required to reach the criterion $\Delta A = 1$, from the kinetic evolution of absorbance $\Delta A \pm \sigma$ for thermo-oxidation of XLPE films at 140 °C.

One recalls that thermal ageing conditions were strictly controlled: first, the air renewal rates of the ovens were controlled and set in the same range (16 – 20 per hour) for all the ageing tests. Second, for reproducibility purposes, different samples with thicknesses of 200 ± 10 µm were aged at each temperature: the samples were placed side by side in the oven, and the exact temperature was measured as close to the samples as possible and controlled before and during the ageing tests. To prevent potential variabilities in thickness, not only between the different tested films but also during thermo-oxidation, the sample thickness was corrected using a reference band in the infrared spectra. For each ageing point, the average of the ΔA absorbance at 1720 cm^{-1}, and the associated standard deviation σ (represented by an error bar on the y-axis) were presented (Figure 1 (a)). Despite these precautions, one clearly observes significant error bars, particularly at 140 °C, reflecting the dispersion of measurements on the aged films and a high heterogeneity of the degradation. In many papers dealing with the monitoring of oxidative degradation by FTIR measurements, authors report only a unique or an average absorbance value [6,7,22,41,45–49].

To account for this deviation, two new kinetic evolutions of the infrared absorbance ΔA - σ and ΔA + σ were drawn. An example of the 140 °C curve is given in Figure 1 (b). Thus, it was possible to graphically determine the time $t_{\alpha,s}$ required to reach a given ΔA absorbance value along with its uncertainty Δt.

Our relative conversion rate methodology, as described above, implies the association of a relative conversion rate α_s with each ΔA absorbance value. Table 1 summarises the values of

the relative conversion rate α_s (0 – 100 %) and the corresponding levels of absorbance ΔA at 1720 cm^{-1} (0 – 2).

Table 1: Relative conversion rate α_s of the thermo-oxidation of XLPE and levels of absorbance ΔA at 1720 cm^{-1} (from 0 to 2).

α_s [%]	0	10	20	30	40	50	60	70	80	90	100
ΔA (1720 cm^{-1})	0	0.2	0.4	0.6	0.8	1.0	1.2	1.4	1.6	1.8	2.0

Then, for each relative conversion rate α_s, the time $t_{\alpha,s} \pm \Delta t$ required to reach the corresponding absorbance level was noted. The linearised Arrhenius law applied to polymer ageing is defined as follows:

$$\ln(t_{\alpha,s}) = \ln(t_0) - \frac{E_a}{RT} \qquad \textit{(Eq. 5)}$$

where t_α *is* the time required to reach the defined oxidation criterion, t_0 is a parameter depending on the processes, E_a *is* the activation energy, R is the universal gas constant and T *is* the absolute temperature. Thus, the times $t_{\alpha,s}$ were plotted on a logarithmic scale versus the inverse of the absolute temperature $\frac{1}{T}$ (from 70 to 160 °C) (Figure 2).

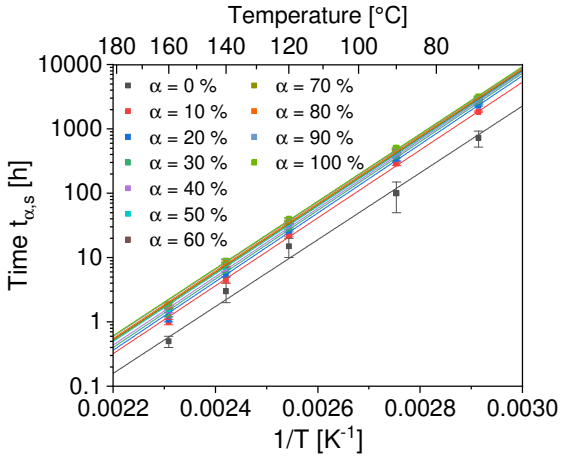

Figure 2: Arrhenius graph of the time required to reach different absorbance values from 0 to 2 for XLPE in the range 70 – 160°C.

Linear fits were determined by considering the uncertainties Δt linked to the determination of the times $t_{\alpha,s}$. The activation energy E_a for each relative conversion rate α_s could then be determined from the slope of the corresponding straight line (according to *Eq. 5*). It can be noted from Figure 2 that the times corresponding to α_s = 0 % were marred by very high experimental errors. This can be explained by the imprecise graphical determination of the

end of the induction period (IP) at each temperature. The activation energy associated with this particular period (highlighted in grey in the following work) will not be analysed and discussed in this paper due to this important error.

To investigate the influence of the raw data chosen for processing on the obtained activation energy, the same methodology was applied to different portions of the curve of the kinetic evolution of infrared absorbance ΔA (Figure 1): first from 0 to 2, then from 0 to 1 and finally from 0 to 0.5. For each studied absorbance curve section, the activation energy E_a was plotted as a function of the relative conversion rate α_s of thermo-oxidation (Figure 3).

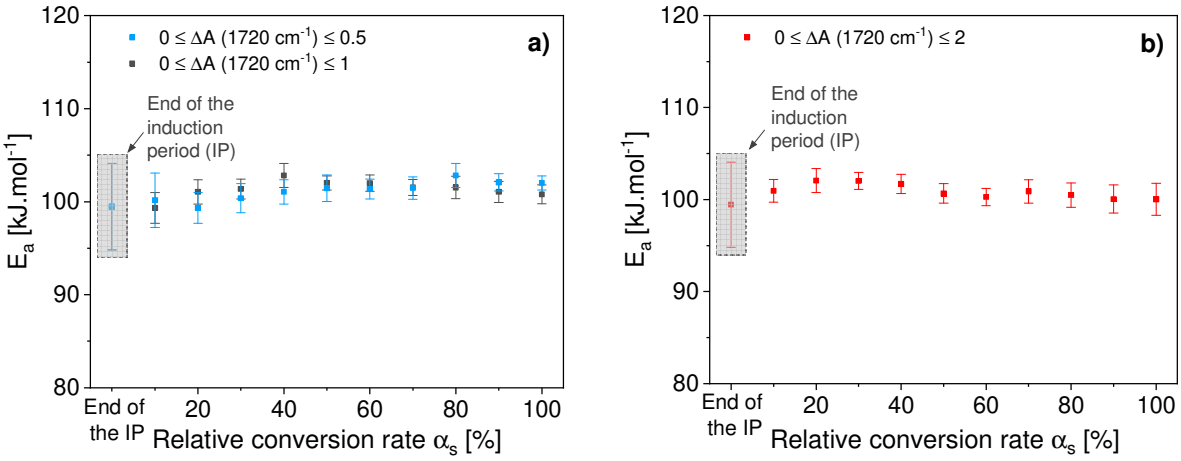

Figure 3: Activation energy versus the relative conversion rate for the thermo-oxidation α_s of XLPE for absorbance values at 1720 cm^{-1} in the ranges (a) 0 – 0.5 and 0 – 1 and (b) 0 – 2.

Due to the important uncertainties shown in Figure 1, the activation energy values should be considered carefully. Nevertheless, trends can be observed. First, one can see from Figure 3 (a) that the values of activation energy were the same regardless of the absorbance curve section studied, from 0 to 0.5 or from 0 to 1. Second, these values of activation energy were constant regardless of the relative conversion rate α_s. In contrast, if ΔA at 1720 cm^{-1} was chosen between 0 and 2, it seems from Figure 3 (b) that for relative conversion rates above 70 % ($\Delta A \geq 1.4$), the values of the activation energies tended to decrease slightly, and the error bars seem to increase. This could be explained by the lack of experimental points between absorbance values of 1 and 2. Moreover, the few experimental points in this domain were marred by high uncertainties resulting from the heterogeneity of the oxidation at these levels of degradation. Another explanation could be the nonlinearity of the Beer-Lambert law at high absorbance and thus at high concentrations [50]. This resulted in high uncertainties in the determination of the times $t_{\alpha,s}$.

Although a different trend seemed to exist for activation energies calculated from high absorbance values, the overlap of error bars associated with the data points leads to the conclusion that the activation energy can be considered independent of the absorbance curve section studied. Thus, an average value of the activation energies determined from three absorbance curve portions was calculated for each relative conversion rate α_s of the reaction (Table 2).

Table 2: Average values of activation energies versus the relative conversion rate, calculated from the three studied absorbance curve sections, for XLPE.

Relative conversion rate α_s [%]	10	20	30	40	50	60	70	80	90	100
Activation energy E_a [kJ.mol^{-1}]	100 ± 3	101 ± 4	101 ± 3	102 ± 2	101 ± 3	101 ± 3	101 ± 2	102 ± 2	101 ± 3	101 ± 3

One can observe that the values of the activation energies were constant regardless of the relative conversion rate.

3.1.1.2. Mechanical tests

In this section, the activation energy of the thermooxidation reaction as a function of "relative conversion rate" α_m was determined from mechanical tests. The loss of XLPE mechanical properties, especially the elongation at break (EAB), during thermo-oxidation between 70 °C and 160 °C was monitored by tensile testing. The force-elongation curves and the results were reported in a previous paper [13]. The kinetic evolution of the elongation at break at the five studied temperatures is displayed in Figure 4. In this case, α_m was calculated with EAB_{t0} = 490 % and EAB_{max} = 50 %, using the same approach used for infrared spectroscopic measurements.

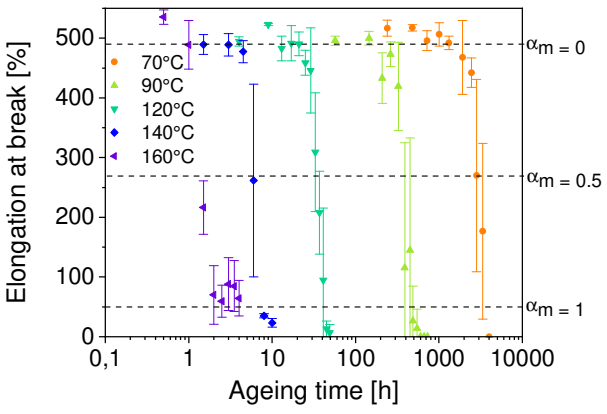

Figure 4: Kinetic evolution of the elongation at break for thermo-oxidation of XLPE at five temperatures (70 – 160 °C).

The elongation at break results in Figure 4 show very large error bars, even larger than those obtained with spectroscopy measurements. Mechanical properties, especially elongation at break, are usually characterised by high error bars due to a large disparity in the results. Indeed, elongation at break is known to be very sensitive to the surface properties of the material, since cracks generated at the surface can rapidly propagate to the sample core and lead to breaking of the material [46]. Thus, because of the heterogeneity of the degradation and depending on the "quantity" of the cracks at the surface of the material and their ability to propagate, the same aged material could fail earlier or later, and this often leads to a high dispersion in the results when testing different samples. In many papers dealing with the monitoring of oxidative degradation by tensile tests, authors report only a single or an average elongation at break value [8,11,32,51–58].

As in section 3.1.1.1., three different curve sections were studied: the first was for elongation at break values from 490 % to 50 %, the second was from 490 % to 200 % and the final was from 490 % to 350 %. For each curve section and for each relative conversion rate α_m (0 – 100 %), the times $t_{\alpha,m}$ and their uncertainties Δt in reaching the corresponding level of elongation at break were noted. By applying the linearised Arrhenius law (*Eq. 5*), the activation energy E_a for each relative conversion rate α_m could then be determined from the slope of the straight lines (Figure 5).

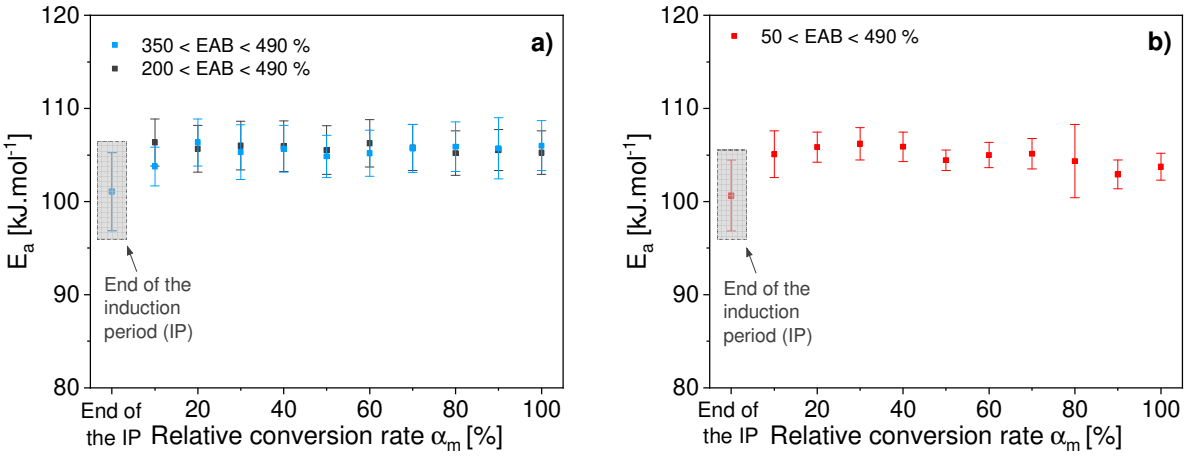

Figure 5: Activation energy versus the relative conversion rate α_m of the thermo-oxidation for XLPE, for EAB in the range (a) 350 – 490 % and 200 – 490 % and (b) 50 – 490 %.

As for spectroscopy results, one can note from Figure 5 (a) that the values of activation energy were the same regardless of the section of the elongation at break curve studied, either from 350 to 490 % or from 200 to 490 %. Second, these values of activation energy were constant regardless of the relative conversion rate α_m. In contrast, for EABs between 490 and 50 % and for relative conversion rates α_m above 70 % (EAB < 105 %), the values of the activation energies tended to decrease slightly. At these levels of degradation, the material was so mechanically damaged that the results do not appear to be consistent with those obtained at lower relative conversion rates. Moreover, the treatment of data on mechanical properties, especially elongation at break, at high deformation often leads to large disparities among the different samples tested. This resulted in high uncertainties in the activation energies.

Although a different trend seems to exist for activation energies calculated from low residual elongation at break values, the overlap of error bars associated with data points leads to the conclusion that the activation energy can be considered independent of the section of the mechanical curve studied. Thus, an average value for the activation energies determined from three sections of the absorbance curve was calculated for each relative conversion rate α_m of the reaction (Table 3).

Table 3: Average values of activation energies versus the relative conversion rate α_m, calculated from the three sections of the mechanical curve, for thermo-oxidation of XLPE.

Relative conversion rate α_m [%]	10	20	30	40	50	60	70	80	90	100
Activation energy E_a [kJ.mol^{-1}]	105 ± 4	106 ± 3	106 ± 4	106 ± 3	105 ± 4	105 ± 4	106 ± 3	105 ± 5	105 ± 4	105 ± 4

For both spectroscopic measurements and tensile test results, the activation energy was constant regardless of the extent of degradation α. Moreover, the uncertainty associated with each activation energy allows us to conclude that activation energies determined from both characterisation techniques (spectroscopic measurements and tensile tests) are similar. These results are not surprising, since a good correlation between the chemical and macromolecular scales was highlighted in a previous paper [13].

3.1.2. Application of the shift factor methodology

In this section, we seek to determine the activation energy of the thermo-oxidation reaction occurring at temperatures ranging from 70 °C to 160 °C and thus to verify the validity of the Arrhenius law over this temperature range, by a different methodology than those applied in the previous section. For this purpose, the time-temperature principle used by Celina and co-workers [33,59–61] was applied. This principle comes from the Williams-Landel-Ferry mathematical model and finds its origin in studies of polymer rheology [62]. First, a reference temperature T_{ref}, usually the lowest experimental temperature (70°C here) is chosen. Then, shift factors a_T are chosen empirically to give the best overall superposition of the data with T_{ref} after multiplying a_T by the experimental times t from spectroscopic data (Figure 1 (a)) and from mechanical tests (Figure 4 (a)) for each temperature data set. These shift factors obey the following Arrhenius law:

$$a_T = \exp\left[\frac{E_a}{R}\left(\frac{1}{T_{réf}} - \frac{1}{T}\right)\right] \qquad (Eq.\ 6)$$

where a_T is the empirical shift factor, E_a *is* the activation energy, R is the gas constant and T_{ref} is the reference temperature. A master curve of the best superposed data is then obtained for spectroscopy data (Figure 6 (a)) and for mechanical data (Figure 6 (b)), with T_{ref} = 70°C.

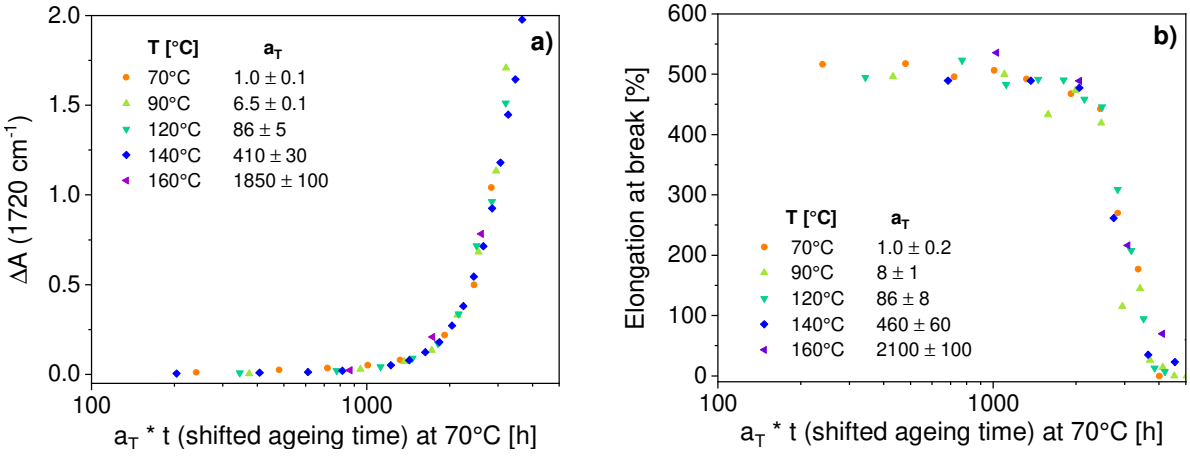

Figure 6: Time-temperature superposition (T_{ref} = 70°C) for XLPE in the range 70 – 160°C for (a) spectroscopic data (0 < ΔA < 2); and (b) mechanical data (490 > EAB > 50 %).

It is necessary to recall that time-temperature superposition is only possible if the shapes of the curves are the same, which implies that all reactions are equally accelerated when the temperature is raised, i.e., the acceleration is constant and independent of the level of degradation [39]. As displayed in Figure 1 (b) and Figure 4 (b), the absorbance and the elongation at break results were plagued with large standard deviations arising from the

limited replicability of the measurements. This resulted in uncertainties for the times t_α for each level of degradation (ΔA or EAB). Thus, it was also necessary for the data superposition to account for this time variability. Consequently, the determined shift factors a_T were also accompanied with uncertainties.

As in the case of the relative conversion rate methodology, to investigate the influence of the data chosen on the resulting activation energy, superposition was also performed on different sections of the curves for the evolution of the absorbance ΔA and the elongation at break EAB.

According to the linearised from of *Eq. 6*, the determined shift factors a_T were plotted on a logarithmic scale versus the inverse of the absolute temperature $\frac{1}{T}$. For each curve section studied, the activation energy E_a could then be determined from the slopes of the straight lines from spectroscopic and mechanical results (Figure 7).

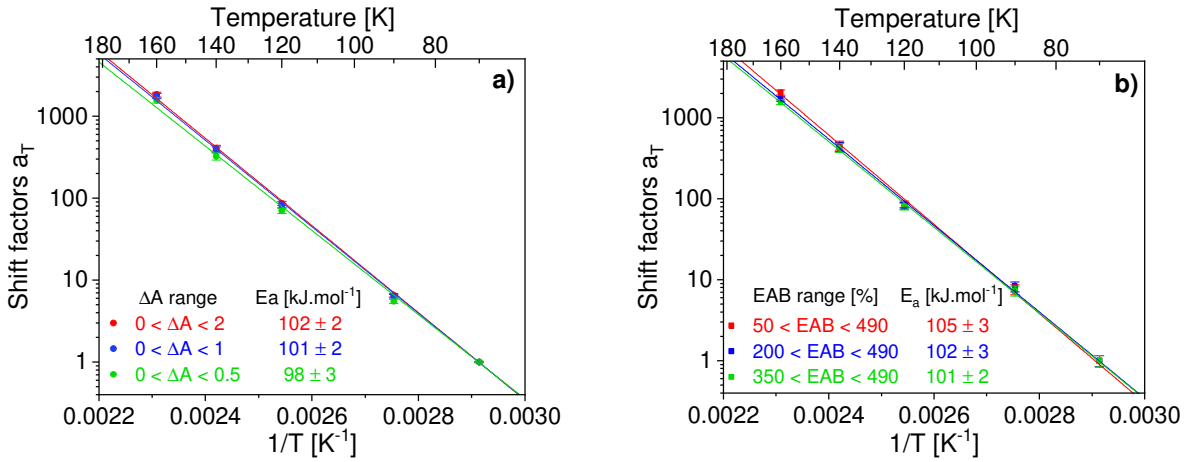

Figure 7: Arrhenius plot of the shift factors a_T determined (a) from spectroscopic results; (b) from mechanical results for thermo-oxidation of XLPE in the temperature range 70 – 160 °C.

A summary of the activation energies in each study range for both spectroscopic and tensile test results is reported in Table 4.

Table 4: Calculated activation energy values according to the chosen study range for both spectroscopic and tensile tests of thermo-oxidation of XLPE.

	Spectroscopic measurements		
Study range	0 < ΔA < 2	0 < ΔA < 1	0 < ΔA < 0.5
E_a [kJ.mol^{-1}]	102 ± 2	101 ± 2	98 ± 3
	Tensile tests		

Study range	50 < EAB > 490 %	200 < EAB < 490 %	350 < EAB < 490 %
E_a [kJ.mol^{-1}]	105 ± 3	102 ± 3	101 ± 2

Taking into consideration the overlap of error bars, one can conclude that the values of activation energies are consistent regardless of the selected data range and the characterisation technique used. The results did not show any significant variation in the activation energy, even for very degraded samples or with high uncertainties arising when monitoring the main oxidation product or the elongation at break. Whatever the applied methodology (relative conversion rate or shift factor methodology), the obtained activation energy values are similar.

However, in the rest of the work, the authors have chosen to process the data only in a certain range to avoid large uncertainties due to a high level of degradation. Thus, the data will only be processed for ΔA values down to an absorbance of 1, where the Beer-Lambert law is fully verified, and only for EAB up to 200 %.

3.2. Investigation of thermo-oxidation at a low temperature

3.2.1. Crosslinked PE

At this step, it is important to remember that the materials used in the cable and wire industry generally experience temperatures of approximately 50 – 70 °C. For this reason, it was necessary to verify the validity of the Arrhenius law at low temperatures and to compare the theoretical and experimental lifetimes of the polymer materials. For this purpose, thermo-oxidation of XLPE samples was also carried out at 50 °C. As for the other temperatures, the aged materials were characterised by spectroscopic measurements and tensile tests. The kinetic evolution of the absorbance at 1720 cm^{-1} at all temperatures, including 50°C, is displayed in Figure 8.

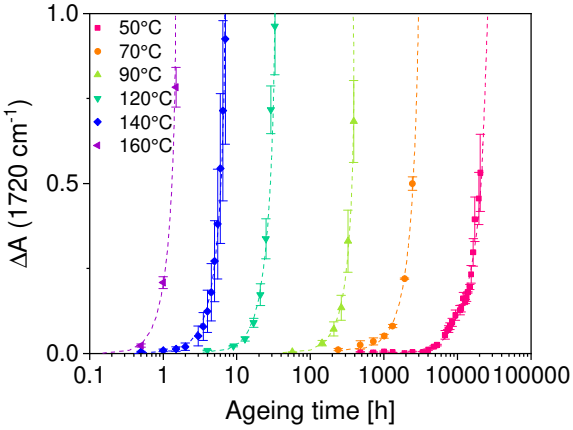

Figure 8: Kinetic evolution of infrared absorbance $\Delta A = A_t - A_{t=0}$ at 1720 cm^{-1} for thermo-oxidation of XLPE films in the temperature range 50 – 160 °C.

At 50°C, the degradation of the material was very slow, as expected, and the results presented here were obtained after approximately 20 500 h of ageing, i.e., at approximately 850 days or approximately 2.3 years. Unfortunately, at this temperature, the XLPE was not damaged enough to observe significant changes in the mechanical properties, particularly in the elongation at break. Thus, this section only focuses on spectroscopic measurements.

First, the aim was to determine the activation energies for each relative conversion rate α_s of the reaction (*cf.* part 3.1.). For that purpose, the times $t_{\alpha,s} \pm \Delta t$ to reach levels of absorbance between 0 and 0.5 were noted. A ΔA absorbance value of approximately 0.5 corresponds to the maximum absorbance level (ΔA_{max}) reached at 50 °C at the date of writing this paper.

Then, these times were plotted versus the inverse of the absolute temperature (*Eq. 5*), and activation energies were determined from the slopes of the corresponding straight lines. To highlight a deviation in the Arrhenius behaviour, the data were fitted separately from 90 to 160 °C and from 50 to 90 °C (Figure 9).

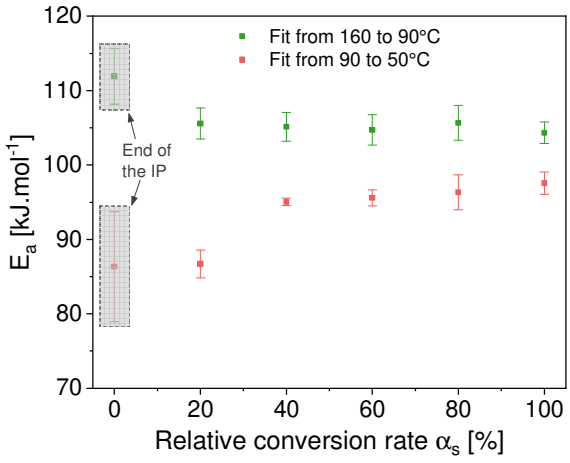

Figure 9: Activation energy versus the relative conversion rate α_s of the thermo-oxidation, from absorbances at 1720 cm^{-1} in the range 0 – 0.5.

To discuss the results, it is necessary to recall that the absorbance range for processing these data is quite restricted (0 to 0.5). Therefore, the determination of the corresponding times was rather imprecise in such a narrow range. Moreover, below an absorbance of 0.2 (α_s < 40 %), one is operating in the transitional regime, that is, the reaction is autoaccelerated, unlike the situation in the permanent regime [63]. This could explain the uncertainties in the activation energy values in this range (0 – 20 %). For this reason, we chose to calculate activation energies at only every 20 % relative conversion rate, i.e., at each 0.1 absorbance increase for all temperatures. By ignoring the data when α_s < 40 %, the fit at the highest temperatures gave an average activation energy of approximately 104 $kJ.mol^{-1}$, and 96 $kJ.mol^{-1}$ was calculated for the lowest temperatures.

Second, we were interested in verifying the validity of the Arrhenius at low temperature (50 °C) by using the shift factor methodology (*cf.* part 3.1.2.). Here, the lowest experimental temperature, i.e., 50 °C, was chosen as the reference temperature. The 70, 90, 120, 140 and 160 °C data sets were manually shifted towards the 50 °C data set (Figure 10 (a)).

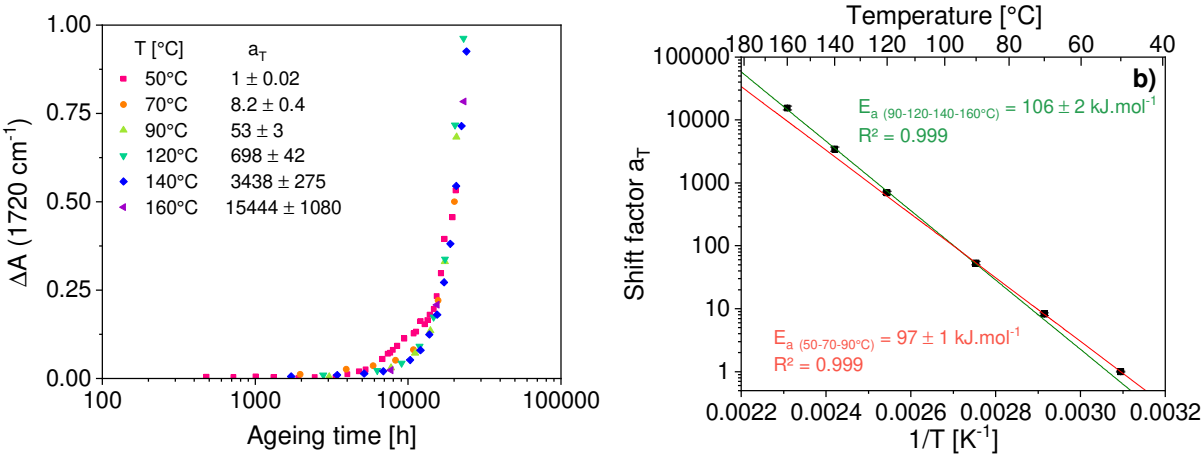

Figure 10: (a) Manual time-temperature superposition of the IR spectroscopic data of XLPE using T_{ref} = 50 °C; (b) Arrhenius plot of the shift factors a_T determined from spectroscopic data of XLPE using a manual time superposition in the range 50 – 160 °C, with T_{ref} = 50 °C.

The first observation is that the total superposition of the 70, 90, 120, 140 and 160 °C curves onto the 50 °C curve is impossible because of the different shape of the 50 °C curve compared to those for other temperatures. However, it is possible to shift the data to superimpose the sections of the curves at which the absorbances were above 0.2, as seen from Figure 10. An

Arrhenius plot of the shift factors associated with this so-called superposition is displayed in Figure 10 (b) from 50 to 160 °C. The results reveal a curvature in the Arrhenius plot, highlighted by separately fitting the data from 90 to 160 °C and the data from 50 to 90 °C. The highest temperature fit (90 – 160 °C) gave an activation energy of 105 ± 2 $kJ.mol^{-1}$, which is of the same order of magnitude as the value obtained in our previous work on the same material [13]. The lowest temperature fit (50 – 90 °C) gave an activation energy of 97 ± 1 $kJ.mol^{-1}$, highlighting the important decrease in the activation energy at low temperatures.

The use of the unsatisfactory superposition shown in Figure 10 (a) to determine activation energies is clearly questionable, since it is normally not consistent with the application of the time-temperature principle. Moreover, as the shift factor methodology is a graphical method, the superposition seems to be at the discretion of the operator, and other superposition choices could have been made. This point will be discussed in forthcoming work. However, we nonetheless used the present superposition for the purpose of estimating the inaccuracy of using the data obtained from high temperatures to predict a lifetime at low temperature, specifically at 50 °C. Thus, an extrapolation of the data using the high temperature fit, i.e., the 90 – 160 °C fit, was performed, and a "theoretical" shift factor of 0.71 was determined for 50 °C. Therefore, if the activation energy was constant over the range 50 – 160 °C, the 50 °C dataset should theoretically be slowed by a factor of 1.4 compared to the current experiment at 50 °C. The experimental times from the 50 °C data set were then shifted by a factor of 1.4 to plot a "theoretical" kinetic curve for reaction at 50 °C (Figure 11).

At this point, it was possible to estimate the inaccuracy of using the data obtained from high temperatures to predict a lifetime at low temperature, specifically at 50 °C. For that purpose, an extrapolation of the data using the high temperature fit, i.e., the 90 – 160 °C fit, was performed, and a theoretical shift factor was determined: a_T (theo. 50°C) = 0.71. Therefore, if the activation energy was constant over the range 50 – 160 °C, the 50 °C dataset should have been slowed by a factor of 75 compared to the ageing at 90 °C, as opposed to the factor of 53 calculated from the current experiment. The experimental times from the 50 °C data set were then shifted by a factor of 1.4 to plot a "theoretical" kinetic curve at 50 °C (Figure 11).

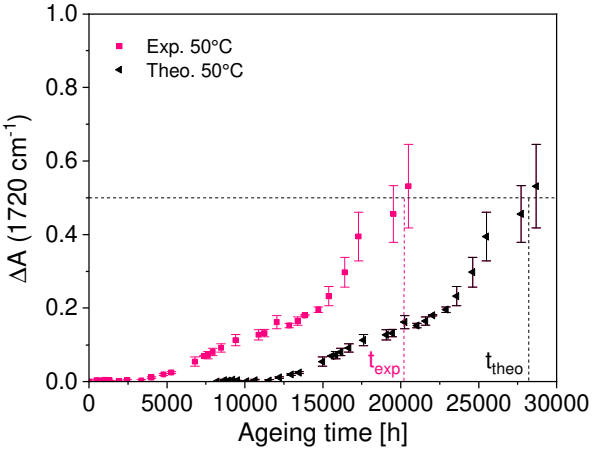

Figure 11: Kinetic evolution of infrared absorbance ΔA at 1720 cm^{-1} for thermo-oxidation of XLPE at 50 °C: experimental and theoretical kinetic curves.

This kinetic absorbance curve corresponds to the curve that should have been obtained for ageing at 50 °C if the activation energy of 106 $kJ.mol^{-1}$ was constant over the range 50 – 160 °C with no deviation at low temperature. It would have taken approximately 28 000 h (approximately 3.2 years) to reach an absorbance value at 1720 cm^{-1} of ΔA = 0.5, versus 20 000 h (approximately 2.3 years) in the current experiment. In this case, the use of the data obtained at high temperatures (90 – 160 °C) to predict a lifetime at 50 °C led to an overestimation of 28 %. To avoid such incorrect results, one of the preconditions for use of the Arrhenius methodology may be to minimise the gap between the lowest experimental temperature and the temperature of interest for which a lifetime prediction is needed.

3.2.2. Crosslinked EPR

To investigate whether the observed deviation at 50 °C was specific to the cross-linked PE, the same approach was carried out with a different material, a cross-linked EPR. This material is an elastomer, unlike XPLE, which is a thermoplastic material. The crystallinity ratios of these two materials have been reported in our previous paper [13]: 46 % for XLPE and 19 % for XLEPR. The DSC thermograms of the first heating of XLPE and XLEPR are displayed in Figure 12.

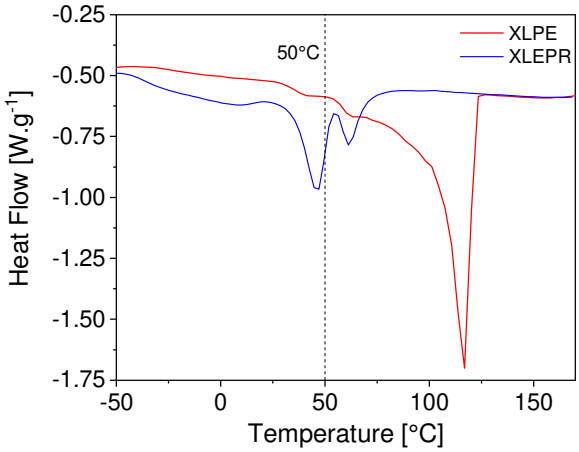

Figure 12: DSC heating thermograms of XLPE and XLEPR.

The melting peak of XLPE was measured as 117 °C. However, no Arrhenius deviation was observed around this transition temperature in our previous work [13]. As shown in Figure 12 and already reported in the literature [4,64], this sample has a very large thickness distribution of crystallites. Indeed, the first crystals began to melt at approximately 50 °C. To test the hypothesis that the deviation observed at 50 °C would be explained by the melting of these first crystals, an XLEPR was studied for comparison. XLEPR exhibits two small melting peaks at 46 °C and 55 °C. In terms of the morphological state of the material, ageing carried out from 50 °C to 160 °C for XLEPR can be considered approximately equivalent to ageing carried out from 120 °C to 160 °C for XLPE, with a major part of the sample in the amorphous phase. The question we wanted to answer was: is a deviation observed for XLEPR at approximately 50 °C, as for XLPE, or is the deviation at 50 °C specific to XLPE?

Thermo-oxidation of XLEPR was carried out from 50 to 160°C, and the material was characterised by infrared spectroscopy and tensile tests, as for XLPE. The kinetic evolution of the formation of the main oxidation product, i.e., carboxylic acids with a band at 1714 cm^{-1}, was monitored at the five temperatures studied (Figure 13 (a)). By applying the same methodology described in section 3.1.1., the times $t_{\alpha,s}$ (corresponding to absorbance levels of ΔA between 0 and 1) were plotted on a logarithmic scale versus the inverse of the absolute temperature, and activation energies were determined. To highlight a deviation in the Arrhenius behaviour, the data were fitted separately from 90 °C to 160 °C and from 50 °C to 90 °C (Figure 13 (b)).

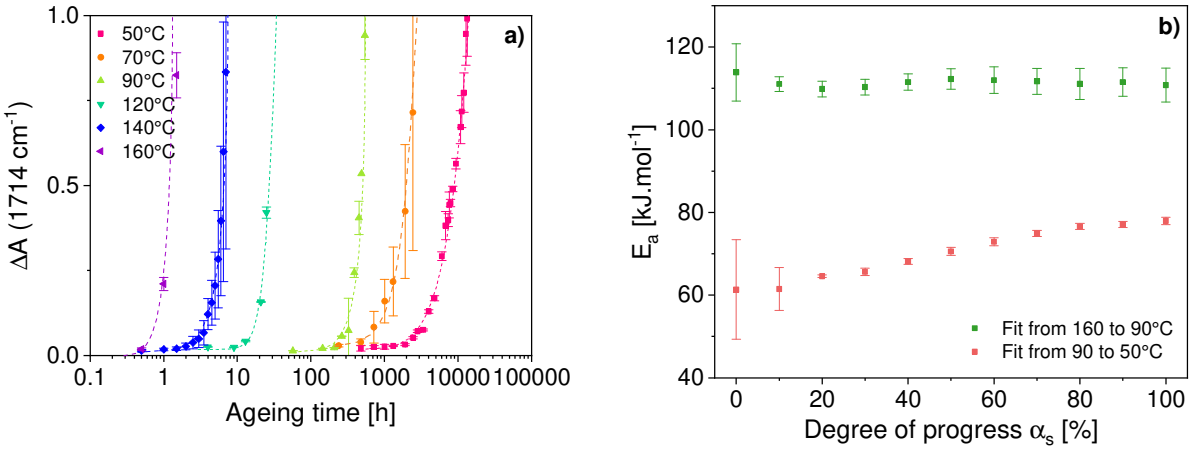

Figure 13: (a) Kinetic evolution of infrared absorbance $\Delta A = A_t - A_{t=0}$ at 1714 cm^{-1} for thermo-oxidation of XLEPR in the temperature range 50 – 160°C; (b) Activation energy of XLEPR versus the relative conversion rate α_s, obtained with data fitted separately from 90 to 160 °C and from 50 to 90 °C.

From the 90 °C to 160°C linear fit, and considering the uncertainties, the activation energy can be considered constant versus the relative conversion rate α_s. The highest temperatures fit (90 – 160 °C) gave an average activation energy of approximately 111 $kJ.mol^{-1}$, and for the lowest temperatures fit (50 – 90 °C) it was approximately 70 $kJ.mol^{-1}$.

To confirm the deviation obtained at low temperatures, we used the shift factor methodology. This latter was applied to the XLEPR spectroscopic data. Manual time-temperature superposition was applied to the data, including the 50 °C data set (Figure 14 (a)).

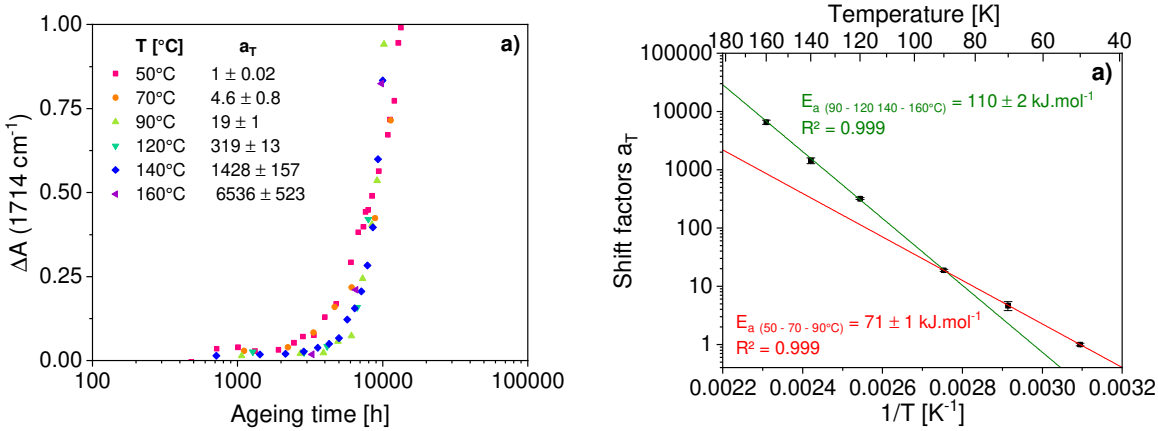

Figure 14: (a) Manual time-temperature superposition of the IR spectroscopic data for thermo-oxidation of XLEPR films in the temperature range 50 – 160 °C using T_{ref} = 50 °C (b) Arrhenius plot of the corresponding empirical shift factors a_T.

As for the case of XLPE, it appears that the 50 °C dataset does not correctly overlap the other temperatures. Nevertheless, an Arrhenius plot of the shift factors a_T determined graphically was then plotted from 50°C to 160°C (Figure 14 (b)). The curvature in the Arrhenius plot was highlighted by separately fitting the data from 90°C to 160°C and the data from 50 to 90 °C. The highest temperature fit gave an activation energy of 110 ± 2 kJ.mol^{-1}, and this value is of the same order of magnitude as the value obtained in our previous work on the same material [13]. The lowest temperature fit (50 – 90 °C) gave an activation energy of 71 ± 1 kJ.mol^{-1}, underlying that there was again an important decrease in the activation energy at low temperatures. Celina et al. [65] reported an Arrhenius deviation for EPDM, with activation energies of 118 kJ.mol^{-1} above 111 °C and 82 kJ.mol^{-1} below 111 °C.

As with XLPE and despite the questionable superposition, this allowed us to highlight the danger of extrapolating high-temperature data for predictions of lifetimes at low temperatures. Indeed, by extrapolating the data using the high temperature fit, i.e., the 90 – 160 °C fit, a "theoretical" shift factor of 0.22 was calculated for 50 °C. The experimental times from the 50 °C data set were then shifted by a factor of 4.5 to plot a "theoretical" kinetic curve at 50 °C (Figure 15).

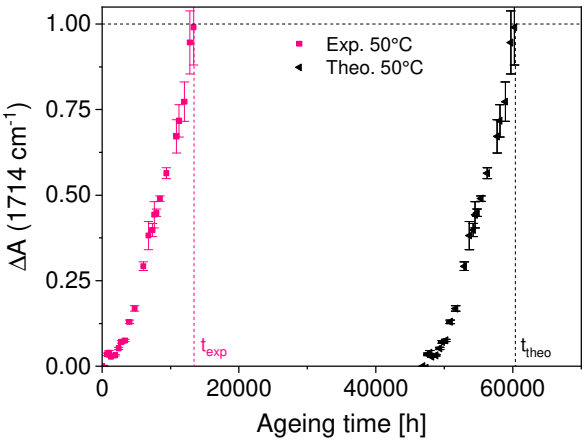

Figure 15: Kinetic evolution of infrared absorbance ΔA at 1714 cm^{-1} for thermo-oxidation of XLEPR at 50 °C: experimental and theoretical kinetic curves.

It would have taken approximately 60 500 h to reach an absorbance value at 1720 cm^{-1} of ΔA = 1, as opposed to the 13 500 h in the current experiment. In this case, the use of the data obtained at high temperatures (90 – 160 °C) to predict a lifetime at 50 °C led to an overestimation of 78 %. This overestimation could be all the more important because it seems to depend strongly on the nature of the materials.

Moreover, this study carried out on an XLEPR material clearly demonstrated that crystallinity does not play a role in the Arrhenius deviation observed at 50 °C, since the same deviation was observed for the XLPE and XLEPR materials and is even more pronounced for the latter.

Although the present materials were not formulated with antioxidants, it is likely that process antioxidants were incorporated by the polymer supplier. The presence of process antioxidants could explain the Arrhenius deviation at low temperatures. The difference in diffusion and/or solubility of antioxidants in polymer matrices has been widely noted in the literature to be dependent on the temperature [23–26,28]. At low temperatures, the antioxidant could be in a "fixed" state, which would reduce its efficiency, thus accelerating the thermo-oxidation mechanism.

Conclusion

The intent of this work was to verify the Arrhenius law in a large temperature domain ranging from 50 to 160 °C for the thermo-oxidation of a cross-linked PE by using two distinct approaches: the relative conversion rate methodology and the shift factor methodology. These two methodologies were applied to two different experimental data sets. The first set was derived from infrared spectroscopic measurements, and the second one was derived from tensile testing. Thus, we demonstrated that (a) the activation energy was constant versus the relative conversion rate, regardless of the characterisation technique used and (b) the activation energy was constant over the range 70 – 160°C. As the melting peak temperature of XLPE was measured at 117 °C, one can conclude that the physical state of the material (semicrystalline or amorphous) does not have an impact on the linearity of the Arrhenius plot.

The evidence of a nonlinearity in the Arrhenius plot at 50 °C was of particular interest. To investigate whether this behaviour was specific to XLPE, a cross-linked EPR was also studied. The physical state of XLEPR at 50 °C can be considered equivalent to that at 120 °C for XLPE. The aim was to determine whether the hypothesis that the small crystals of XLPE, which begin to melt at approximately 25 – 50 °C, could be responsible for the observed Arrhenius deviation at low temperatures. However, the same deviation was highlighted for XLEPR. This result proved that the crystallinity cannot explain the Arrhenius deviation observed at low temperatures. These low temperatures (50 – 70 °C) are all the more important, as they are close to those the material experiences due to natural ageing during use.

The lifetime at 50 °C calculated from extrapolation of high temperature results was overestimated by 28 % for XLPE and 78 % for XLEPR, as compared to the experimental results obtained at 50 °C. This overestimation serves as a warning about the reliability of such Arrhenius predictions for industrial applications.

Acknowledgements

The authors wish to thank Nexans for the financial support and Jean-Luc Gardette for scientific discussions.

References

[1] S.M. Tamboli, S.T. Mhaske, D.D. Kale, Crosslinked polyethylene, Indian J. Chem. Technol. 11 (2004) 853–864.

[2] S.F. Chabira, M. Sebaa, C. G'sell, Oxidation and crosslinking processes during thermal aging of low-density polyethylene films, J. Appl. Polym. Sci. 24 (2011) 5200–5208. https://doi.org/10.1002/app.34080.

[3] A. Perthué, P.-O. Bussière, M. Baba, J.-F. Larche, J.-L. Gardette, S. Therias, Correlation between water uptake and loss of the insulating properties of PE/ATH composites used in cables applications, Polym. Degrad. Stab. 127 (2016) 79–87. https://doi.org/10.1016/j.polymdegradstab.2016.01.020.

[4] L. Boukezzi, A. Boubakeur, C. Laurent, M. Lallouani, Observations on structural changes under thermal ageing of cross-linked polyethylene used as power cables insulation, Iran. Polym. J. 17 (2008) 611–624.

[5] G. Rapp, J. Tireau, P.-O. Bussiere, J.-M. Chenal, F. Rousset, L. Chazeau, J.-L. Gardette, S. Therias, Influence of the physical state of a polymer blend on thermal ageing, Polym. Degrad. Stab. 163 (2019) 161–173. https://doi.org/10.1016/j.polymdegradstab.2019.03.006.

[6] F. Delor, G. Teissedre, M. Baba, J. Lacoste, Ageing of EPDM—2. Role of hydroperoxides in photo- and thermo-oxidation, Polym. Degrad. Stab. 60 (1998) 321–331. https://doi.org/10.1016/S0141-3910(97)00087-6.

[7] K. Anandakumaran, D.J. Stonkus, Assessment of oxidative thermal degradation of crosslinked polyethylene and ethylene propylene rubber cable insulation, Polym. Eng. Sci. 32 (1992) 1386–1393.

[8] A.K. Bhowmick, J.R. White, Thermal, UV- and sunlight ageing of thermoplastic elastomeric natural rubber-polyethylene blends, J. Mater. Sci. 37 (2002) 5141–5151.

[9] K.E. Figueroa, Thermoanalytical study of an aged XLPE-pipe, Thermochim. Acta. 114 (1987) 115–124.

[10] R. Sarathi, S. Das, C.R. Anil Kumar, R. Velmurugan, Analysis of failure of crosslinked polyethylene cables because of electrical treeing: A physicochemical approach, J. Appl. Polym. Sci. 92 (2004) 2169–2178. https://doi.org/10.1002/app.20200.

[11] F. Delor-Jestin, J. Lacoste, N. Barrois-Oudin, C. Cardinet, J. Lemaire, Photo-, thermal and natural ageing of ethylene–propylene–diene monomer (EPDM) rubber used in automotive applications. Influence of carbon black, crosslinking and stabilizing agents,

Polym. Degrad. Stab. 67 (2000) 469–477. https://doi.org/10.1016/S0141-3910(99)00147-0.

[12] N.S. Tomer, F. Delor-Jestin, L. Frezet, J. Lacoste, Oxidation, Chain Scission and Cross-Linking Studies of Polysiloxanes upon Ageings, Open J. Org. Polym. Mater. 02 (2012) 13–22. https://doi.org/10.4236/ojopm.2012.22003.

[13] C. Blivet, J.-F. Larché, Y. Israëli, P.-O. Bussière, J.-L. Gardette, Thermal oxidation of cross-linked PE and EPR used as insulation materials: Multi-scale correlation over a wide range of temperatures, Polym. Test. 93 (2021) 106913. https://doi.org/10.1016/j.polymertesting.2020.106913.

[14] L. Audouin, X. Colin, B. Fayolle, J. Verdu, Sur l'utilisation de la loi d'Arrhenius dans le domaine du vieillissement des polymères, Matér. Tech. 95 (2007) 167–177. https://doi.org/10.1051/mattech:2008001.

[15] M.C. Celina, K.T. Gillen, E.R. Lindgren, Nuclear Power Plant Cable Materials: Review of Qualification and Currently Available Aging Data for Margin Assessments in Cable Performance, (2013) 144.

[16] M. Celina, K.T. Gillen, R.A. Assink, Accelerated aging and lifetime prediction: Review of non-Arrhenius behaviour due to two competing processes, Polym. Degrad. Stab. 90 (2005) 395–404.

[17] J.W. Tamblyn, G.C. Newland, Induction period in the aging of polypropylene, J. Appl. Polym. Sci. 9 (1965) 2251–2260. https://doi.org/10.1002/app.1965.070090617.

[18] N.C. Billingham, D.C. Bott, A.S. Manke, Application of thermal analysis methods to oxidation and stabilisation of polymers, in: Dev. Polym. Degrad. — 3, Applied Science Publishers, N. Grassie, London, 1981: pp. 63–100.

[19] E. Kramer, J. Koppelmann, Measurement of oxidation stability of polyolefins by thermal analysis, Polym. Degrad. Stab. 16 (1986) 261–275.

[20] J.B. Howard, DTA for control of stability in polyolefin wire and cable compounds, Polym. Eng. Sci. 13 (1973) 429–434. https://doi.org/10.1002/pen.760130606.

[21] J.B. Howard, H.M. Gilroy, Some observations on the long-term behavior of stabilized polyethylene, Polym. Eng. Sci. 15 (1975) 268–271. https://doi.org/10.1002/pen.760150406.

[22] V. Langlois, L. Audouin, J. Verdu, P. Courtois, Thermooxidative aging of crosslinked linear polyethylene: Stabilizer consumption and lifetime prediction, Polym. Degrad. Stab. 40 (1993) 399–409. https://doi.org/10.1016/0141-3910(93)90150-H.

[23] J.Y. Moisan, Diffusion des additifs du polyethylene—I Influence de la nature du diffusant, Eur. Polym. J. 16 (1980) 979–987. https://doi.org/10.1016/0014-3057(80)90180-9.

[24] R.-J. Roe, H.E. Bair, C. Gieniewski, Solubility and diffusion coefficient of antioxidants in polyethylene, J. Appl. Polym. Sci. 18 (1974) 843–856. https://doi.org/10.1002/app.1974.070180319.

[25] H. Zweifel, R.D. Maier, M. Schiller, Plastics Additives Handbook, 6th Edition, Hanser Publishers, Munich, 2009.

[26] E. Földes, B. Turcsányi, Transport of small molecules in polyolefins. I. Diffusion of lrganox 1010 in polyethylene, J. Appl. Polym. Sci. 46 (1992) 507–515.

[27] J.-Y. Moisan, Etude de la migration et de la solubilité des antioxydants dans le polyéthylène, Ann. Telecommun. 34 (1979) 7.

[28] N.C. Billingham, P.D. Calvert, A.S. Manke, Solubility of phenolic antioxidants in polyolefins, J. Appl. Polym. Sci. 26 (1981) 3543–3555. https://doi.org/10.1002/app.1981.070261103.

[29] H.E. Bair, Exudation of an antioxidant additive from thin polyethylene films, Polym. Eng. Sci. 13 (1973) 435–439.

[30] N. Khelidj, X. Colin, L. Audouin, J. Verdu, C. Monchy-Leroy, V. Prunier, Oxidation of polyethylene under irradiation at low temperature and low dose rate. Part II. Low temperature thermal oxidation, Polym. Degrad. Stab. 91 (2006) 1598–1605. https://doi.org/10.1016/j.polymdegradstab.2005.09.012.

[31] J. Wise, K.T. Gillen, R.L. Clough, An ultrasensitive technique for testing the Arrhenius extrapolation assumption for thermally aged elastomers, Polym. Degrad. Stab. 49 (1995) 403–418.

[32] K.T. Gillen, R.L. Clough, J. Wise, Prediction of elastomer lifetimes from accelerated thermal-aging experiments, in: Polym. Durab., American Chemical Society, Washington, DC, 1996: pp. 557–575. https://doi.org/10.1021/ba-1996-0249.ch034.

[33] K.T. Gillen, M. Celina, R.L. Clough, Limitations of the Arrhenius methodology, in: 26th Water Reactor Safety Information Meeting, Maryland, United States, 1998.

[34] K.T. Gillen, R.L. Clough, M. Celina, J. Wise, G.M. Malone, Proceedings of the 23rd Water Reactor Safety Information Meeting, in: NUREGCP-0149, Bethesda, Maryland, 1995: pp. 133–151.

[35] J. Wise, K.T. Gillen, R.L. Clough, Quantitative model for the time development of diffusion-limited oxidation profiles, Polymer 38 (1997) 1929–1944.

[36] K.T. Gillen, K.E. Mead, Predicting life expectancy and simulating age of complex equipment using accelerated aging techniques, Sandia Laboratories Report, Albuquerque, New Mexico, 1980.

[37] K.T. Gillen, R.L. Clough, Time-temperature-dose rate superposition: A methodology for extrapolating accelerated radiation aging data to low dose rate conditions, Polym. Degrad. Stab. 24 (1989) 137–168. https://doi.org/10.1016/0141-3910(89)90108-0.

[38] IEC Central Office, International Standard IEC 60216-4-2. Electrical insulating materials - Thermal endurance properties. Part 4-2: Ageing ovens - Precision ovens for use up to 300°C, (2000).

[39] P. Bracco, L. Costa, M.P. Luda, N. Billingham, A review of experimental studies of the role of free-radicals in polyethylene oxidation, Polym. Degrad. Stab. 155 (2018). https://doi.org/10.1016/j.polymdegradstab.2018.07.011.

[40] K. Jacobson, L. Costa, P. Bracco, N. Augustsson, B. Stenberg, Effects of microtoming on oxidation of ultra high molecular weight polyethylene (UHMWPE), Polym. Degrad. Stab. 73 (2001) 141–150. https://doi.org/10.1016/S0141-3910(01)00080-5.

[41] R. Yang, Y. Liu, J. Yu, K. Wang, Thermal oxidation products and kinetics of polyethylene composites, Polym. Degrad. Stab. 91 (2006) 1651–1657. https://doi.org/10.1016/j.polymdegradstab.2005.12.013.

[42] K. Möller, T. Gevert, A. Holmström, Examination of a low density polyethylene (LDPE) film after 15 years of service as an air and water vapour barrier, Polym. Degrad. Stab. 73 (2001) 69–74. https://doi.org/10.1016/S0141-3910(01)00067-2.

[43] IEC Central Office, International Standard IEC 60811-501. Electric and optical fibre cables – Test methods for non-metallic materials - Part 501: Mechanical tests – Tests for determining the mechanical properties of insulating and sheathing compounds, (2011).

[44] P. Musto, G. Ragosta, M. Abbate, G. Scarinzi, Photo-oxidation of high performance epoxy networks: Correlation between the molecular mechanisms of degradation and the viscoelastic and mechanical response, Macromolecules. 41 (2008) 5729–5743. https://doi.org/10.1021/ma8005334.

[45] B. Fayolle, L. Audouin, J. Verdu, A critical molar mass separating the ductile and brittle regimes as revealed by thermal oxidation in polypropylene, Polymer. 45 (2004) 4323–4330. https://doi.org/10.1016/j.polymer.2004.03.069.

[46] X. Liu, J. Zhao, R. Yang, R. Iervolino, S. Barbera, A novel in-situ aging evaluation method by FTIR and the application to thermal oxidized nitrile rubber, Polym. Degrad. Stab. 128 (2016) 99–106. https://doi.org/10.1016/j.polymdegradstab.2016.03.008.

[47] E. Richaud, F. Farcas, B. Fayolle, L. Audouin, J. Verdu, Accelerated ageing of polypropylene stabilized by phenolic antioxidants under high oxygen pressure, J. Appl. Polym. Sci. 110 (2008) 3313–3321. https://doi.org/10.1002/app.28915.

[48] M. Elvira, P. Tiemblo, J.M. Gómez-Elvira, Changes in the crystalline phase during the thermo-oxidation of a metallocene isotactic polypropylene. A DSC study, Polym. Degrad. Stab. 83 (2004) 509–518. https://doi.org/10.1016/j.polymdegradstab.2003.08.010.

[49] F. Djouani, B. Patel, E. Richaud, B. Fayolle, J. Verdu, Antioxidants loss kinetics in polyethylene exposed to model ethanol based biofuels, Fuel. 93 (2012) 502–509. https://doi.org/10.1016/j.fuel.2011.10.064.

[50] A.Y. Tolbin, V.E. Pushkarev, L.G. Tomilova, N.S. Zefirov, Threshold concentration in the nonlinear absorbance law, Phys. Chem. Chem. Phys. 19 (2017) 12953–12958. https://doi.org/10.1039/C7CP01514C.

[51] M. Celina, K.T. Gillen, R.L. Clough, Inverse temperature and annealing phenomena during degradation of crosslinked polyolefins, Polym. Degrad. Stab. 61 (1998) 231–244. https://doi.org/10.1016/S0141-3910(97)00142-0.

[52] M.S. Rabello, J.R. White, Crystallization and melting behaviour of photodegraded polypropylene– 1. Chemi-crystallization, Polymer. 38 (1997) 6379–638.

[53] M. Le Huy, G. Evrard, Methodologies for lifetime predictions using Arrhenius and WLF models, Macromolecual Mater. Eng. 261/262 (1998) 135–142.

[54] Y. Sun, S. Luo, K. Watkins, C.P. Wong, Electrical approach to monitor the thermal oxidation aging of carbon black filled ethylene propylene rubber, Polym. Degrad. Stab. 86 (2004) 209–215. https://doi.org/10.1016/j.polymdegradstab.2004.04.013.

[55] R. Clavreul, Evolution of ethylene propylene copolymers properties during ageing, Nucl. Instrum. Methods Phys. Res. Sect. B Beam Interact. Mater. At. 131 (1997) 192–197. https://doi.org/10.1016/S0168-583X(97)00139-0.

[56] P.V. Zamotaev, Z. Strel'tsova, L. Matisova-Rychla, I. Chodak, Thermo-oxidation of crosslinked polyethylene: Influence of the antioxidant, Polym. Degrad. Stab. 42 (1993) 167–174. https://doi.org/10.1016/0141-3910(93)90109-V.

[57] K.T. Gillen, R. Bernstein, M. Celina, Challenges of accelerated aging techniques for elastomers lifetimes predictions, Rubber Chem. Technol. 88 (2015) 1–27. https://doi.org/10.5254/rct.14.85930.

[58] T. Seguchi, K. Tamura, T. Ohshima, A. Shimada, H. Kudoh, Degradation mechanisms of cable insulation materials during radiation–thermal ageing in radiation environment,

Radiat. Phys. Chem. 80 (2011) 268–273. https://doi.org/10.1016/j.radphyschem.2010.07.045.

[59] M. Celina, J. Wise, D.K. Ottesen, K.T. Gillen, R.L. Clough, Correlation of chemical and mechanical property changes during oxidative degradation of neoprene, Polym. Degrad. Stab. 68 (2000) 171–184.

[60] K.T. Gillen, R. Bernstein, R.L. Clough, M. Celina, Lifetime predictions for semi-crystalline cable insulation materials: I. Mechanical properties and oxygen consumption measurements on EPR materials, Polym. Degrad. Stab. 91 (2006) 2146–2156. https://doi.org/10.1016/j.polymdegradstab.2006.01.009.

[61] K.T. Gillen, R. Bernstein, D.K. Derzon, Evidence of non-Arrhenius behaviour from laboratory aging and 24-year field aging of polychloroprene rubber materials, Polym. Degrad. Stab. 87 (2005) 57–67. https://doi.org/10.1016/j.polymdegradstab.2004.06.010.

[62] M.L. Williams, R.F. Landel, J.D. Ferry, The temperature dependence of relaxation mechanisms in amorphous polymers and other glass-forming liquids, J. Am. Chem. Soc. 77 (1955) 3701–3707. https://doi.org/10.1021/ja01619a008.

[63] J. Verdu, Oxydative Ageing of Polymers, ISTE Ltd and John Wiley & Sons, Inc., Great Britain (UK) and United States of America (USA), 2012.

[64] L. Boukezzi, A. Boubakeur, C. Laurent, M. Lallouani, DSC study of artificial thermal aging of XLPE insulation cables, Int. Conf. Solid Dieletrics Winch. UK. (2007) 146–149.

[65] K.T. Gillen, M. Celina, The wear-out approach for predicting the remaining lifetime of materials, Polym. Degrad. Stab. 71 (2000) 15–30.